TEFLU Computational Benchmark
ASCHLIM Project WP 2

WP coordinator: L. Maciocco*

*CRS4 (Centre for Advanced Studies, Research and Development in Sardinia)

ENEA (Institute for New Technologies, Energy and Environment, Italy)

FZJ (Juelich Research Centre, Germany)

FZK-IRS (Karlsruhe Research Centre – Institute for Reactors Safety, Germany)

LAESA (Energy Amplifier Laboratory, Spain)

NRG (The Netherlands)

UPV (University of the Basque Countries, Spain)

December 2002

Abstract

This document summarises the results obtained for the WP2 (TEFLU benchmark) of the ASCHLIM project. The main task of the benchmark was the assessment of the limitations of an eddy viscosity approach for HLM flows.

The test case set-up and boundary conditions are described, highlighting some problems coming from the definition of inlet boundary conditions for turbulence quantities. A summary of the approaches followed and of the results obtained by each participant is then reported, making reference to the full reports annexed in the Appendix.

Some general conclusions are drawn, as a synthesis of the conclusions reached by every participant.

The main conclusion is that an approach based on the Reynolds analogy with $Pr_t \sim 1$ is not able to simulate the correct temperature spreading rate of the TEFLU experiment, and, more in general, it is unsuitable for low Peclet number flows. Higher values of Pr_t, possibly as a function of local flow characteristics should be used, or higher order methods, not based on the Reynolds analogy.

The tendency of two-equation models to overestimate the velocity spreading-rate is confirmed, even if definite conclusions about this point can not be drawn, due to the uncertainties in the inlet turbulence conditions.

Contents

1. Introduction

The TEFLU experiment was performed at the Karlsruhe Research Centre (FZK) in order to study the thermal-fluid dynamic behaviour of a hot sodium jet in different flow regimes [1]. It has been chosen in the framework of the ASCHLIM project as a benchmark for testing the capabilities of Computational Fluid Dynamics (CFD) codes at simulating Heavy Liquid Metal (HLM) turbulent flows with heat transfer.

In all two-equations turbulence models (which are the most commonly used in industrial CFD simulations), as well as in the Reynolds Stress model, the turbulent heat transport is modelled on the basis of an analogy with the turbulent transport of momentum (Reynolds analogy). In fact, the turbulent heat diffusion coefficient is assumed to be proportional to the turbulent viscosity through an empirical constant (the turbulent Prandtl number Pr_t). On the basis of the experience with fluids with Prandtl number of order unity, this coefficient is usually set to a value of 0.9, which means that turbulent transport of momentum and heat are almost equivalent.

However, for low Prandtl number fluids, like liquid metals, the approach based on the Reynolds analogy can be incorrect, especially in flows (or regions of the flow) where the Reynolds number is not very high, and the thermal conduction becomes comparable to the turbulent thermal diffusion (low-Peclet-number flows). In this case, a constant value of Pr_t set to 0.9 could lead to an overestimation of the turbulent heat fluxes. The problem can be approached by using higher values of Pr_t, even variable with the flow characteristics, or to abandon the Reynolds analogy and use higher order methods and solve the transport equation for the turbulent heat fluxes. Both approaches has been used within the TEFLU benchmarking activity (see Sec. 4).

Beside the problem of Pr_t, which is mainly related to the simulation of liquid metal flows, two more difficulties arise in the simulation of the TEFLU benchmark. The first concerns the intrinsic limitations of turbulence models, which are related to the type of flow to be simulated. The second is related to the inlet boundary conditions for the turbulence quantities.

In fact, it is well known that almost all the various versions of two-equations models give rise to the so-called round-jet anomaly [2]. Almost all two-equation model (Standard, Low-Re and RNG k-ε models as well as the k-ω model) predict a too high jet spreading-rate. The problem is claimed to be solved in some modified versions of the k-ε model like the Chen k-ε [3] [4] and the Realisable k-ε [5].

The second problem is related to the fact that the TEFLU experimental apparatus allowed the measurement of velocity, temperature and temperature fluctuations. No experimental data are available for velocity fluctuations. This is a problem for the definition of turbulence boundary conditions for the numerical simulation, which makes the evaluation of the capability of turbulence models at predicting the correct jet spreading rate quite questionable.

Despite the above-mentioned problems, some useful conclusions can be drawn from the TEFLU benchmark, as described further on.

2. List of Participants

The institutes and people involved in to the benchmark exercise are listed below

- **CRS4-CFDC** (Centre for Advanced Studies, Research and Development in Sardinia – Computational Fluid Dynamics and Combustion Area, Italy);

  – I. Di Piazza, M. Mulas.

- **CRS4-EA**(Centre for Advanced Studies, Research and Development in Sardinia - Energy Amplifier Group, Italy);

  – L. Maciocco; S. Buono, L. Sorrentino.

- **ENEA** (Institute for New Technologies, Energy and Environment, Italy);

  – G. Mercurio, V.V. Anissimov, V.I. Mikhin, Y.I. Gritsaev.

- **FZJ** (Juelich Research Centre, Germany);

  – J. Wolters.

- **FZK-IRS** (Karlsruhe Research Centre – Institute for Reactors Safety, Germany);

  – L.N. Carteciano, G. Grötzbach.

- **LAESA** (Energy Amplifier Laboratory, Spain);

  – A. Abánades, A. Castro.

- **NRG** (The Netherlands);

  – N.B. Siccama, E.M.J. Komen, H. Koning, F. Roelofs.

- **UPV** (University of the Basque Countries, Spain);

  – A. Peña, J. Merino, A. Etxegia

3. Benchmark Description

3.1. Test case layout

Figure 1 shows a sketch of the test case (see [1] for a more detailed description of the TEFLU experimental apparatus). A central hot stream (*jet*) is injected in a flow with lower velocity and temperature (*co-flow*) coming out from a perforated 16.7 mm thick block (*jet block*) consisting of 158 holes of diameter d= 7.2 mm arranged in a triangular pitch of 8.2 mm.

Experimental measurements are available at different axial distances from the jet inlet. For our benchmarking purpose, only sections at x/d = 6, 12, 20 and 40 has be considered. At every position, velocity, temperature and temperature fluctuations measurements are available, starting from the axis up to a radius of about 40 mm, with a pitch of about 2 mm. Due to the position of the thermocouples in the probe, experimental measurements of temperatures and temperature fluctuations are available at one jet diameter upstream with respect to velocity data (hence, at sections 5, 11, 19, 39).

Experiments showed that the flow can be considered axial-symmetric at a distance x/d = 6 from the jet block, where radial profiles start to be self-similar [1].. Therefore, a computational domain starting from this section has been considered, where suitable inlet boundary conditions are applied (see Sec.3.3).
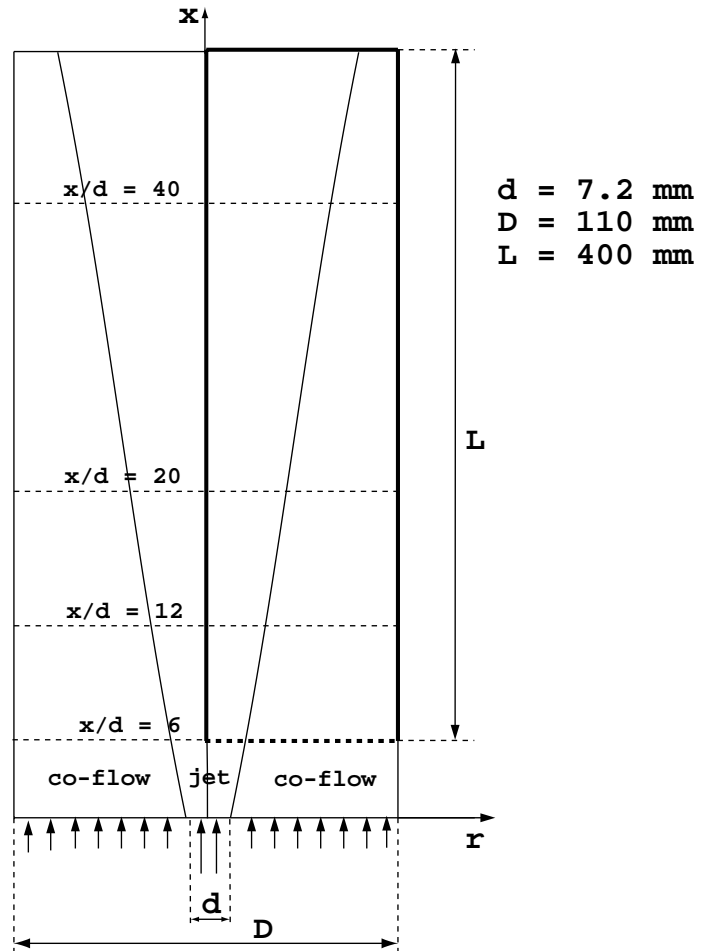
Figure 1- Sketch of the TEFLU test case. The calculation domain is traced with thick lines.

3.2. Experimental conditions and list of test cases

Three different flow regimes (forced flow, buoyant flow and plume), corresponding to different values of the jet and co-flow velocity and temperature. These are listed in Table 1, where the subscripts *cf* and *j* refer to co-flow and jet characteristics respectively, and Δu_j and ΔT_j are the difference between the jet and the co-flow velocity and temperature, namely

$$\Delta \bar{u}_j = \bar{u}_j - \bar{u}_{cf} \tag{1}$$

$$\Delta \overline{T}_j = \overline{T}_j - \overline{T}_{cf} \tag{2}$$

The flow characteristic numbers are the following:

$$\text{Re}_{cf} = \frac{\bar{u}_{cf} D}{\nu_0} \qquad\qquad \textit{co-flow Reynolds number}$$

$$\text{Re}_j = \frac{\bar{u}_j d}{\nu_0} \qquad\qquad \textit{jet Reynolds number}$$

5

$$Fr_j = \frac{\rho_j(\overline{u_j^2} - \overline{u_{cf}^2})}{g(\rho_{cf} - \rho_j)d}$$

densimetric Froude number

Sodium physical properties at the co-flow temperature are reported in Table 2. Variable properties as a function of temperature has been assigned for the benchmark calculations (see 0).

Table 1 - Experimental conditions.

Experiment	$\overline{u}_{cf}$ (m/s)	$\overline{T}_{cf}$ (^{o}C)	Re_{cf}	$\Delta\overline{u}_j$ (m/s)	$\Delta\overline{T}_j$ (^{o}C)	ρ_j (Kg/m^3)	Re_j	Fr_j	$\dot{m}_{tot}$ (Kg/s)
a) forced jet	0.05	300	1.4×10^4	0.50	30	872.87	1.01×10^4	521	0.436
b) buoyant jet	0.1	300	2.8×10^4	0.33	25	874.05	7.9×10^3	365	0.848
c) plume	0.1	300	2.8×10^4	0.17	75	862.16	4.96×10^3	43.1	0.842

Table 2 - Physical properties of sodium at T = 300 ^{o}C

Property	Symbol [units]	Value for T = 300 ^{o}C
Density	ρ [Kg/m^3]	880
Thermal conductivity	λ [W/m/K]	76.58
Molecular viscosity	μ [Kg/m/s]	3.446×10^{-4}
Specific heat at constant pressure	C_p [J/Kg/K]	1304.5
Prandtl number	Pr	5.87×10^{-3}
Peclet number (for Re = 10^4)	Pe = Re Pr	≈ 60

3.3. Computational domain and boundary conditions

The flow is considered axisymmetric, thus only a small sector of the pipe with cyclic conditions is simulated (or a 2D domain in cylindrical coordinates). Figure 2 shows the map of the boundary conditions on the computational domain. The inlet boundary condition lies in correspondence of section at x/d = 6. Profiles of the normal velocity component, as well as temperature profiles, have been applied on the basis of experimental measurement in this section, using linear interpolation between the given data points. Radial velocity components have been considered negligible.
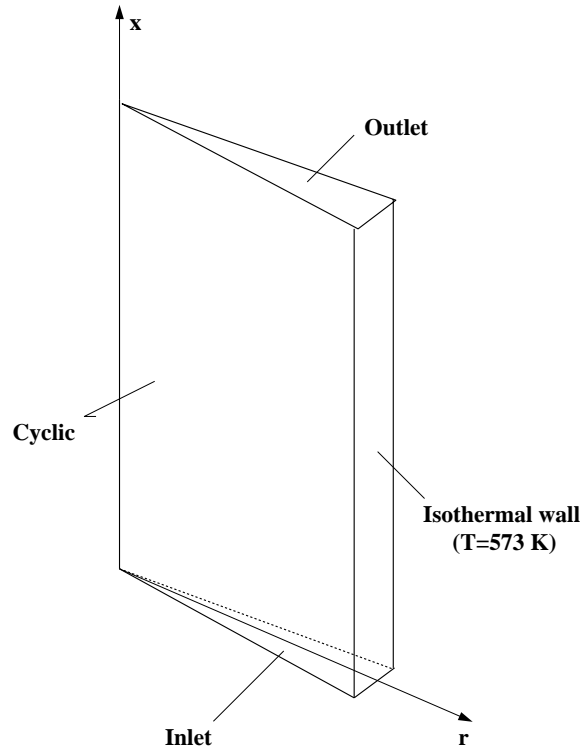
Figure 2 - Boundary conditions.

Velocity profiles have been deduced from the actual experimental data through polynomial interpolation. Experimental data are available in a entire channel cross section, in a range -5 < x/d < 5, approximately. The two sides of the profiles are not completely symmetrical with respect to the axis, so they have been superimposed to obtain an axisymmetric interpolating profile. The value of the final points of each profile (at x/d = 7.6) has been set in order to verify the prescribed mass flow rate (having assumed a linear profile between the last two points). The values at r/d=0 are the actual experimental value measured in the centreline. In order to have both velocity and temperature data in the same section (as explained above, temperature measurements are not directly available in section x/d = 6) inlet temperature profiles have been obtained interpolating the profiles of the adjacent sections.

Inlet profiles of velocity, temperature are shown in Figure 3, Figure 4 and Figure 5, compared with the experimental data. Temperature fluctuation profiles are shown in Figure 6. In some cases it was found that temperature measurements in section x/d=7 were abnormally low. In these cases, data relative to this section have been excluded from the interpolation procedure. Radial velocity components has been considered negligible.
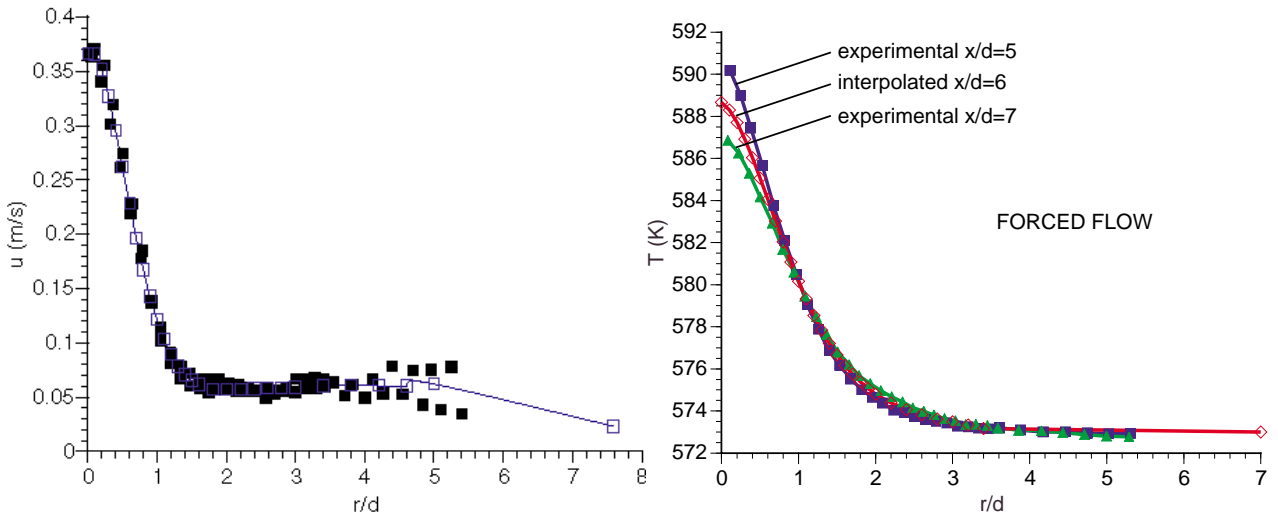
Figure 3 - Inlet velocity (left) and temperature (right) profiles for case a (forced flow). Solid symbols refer to actual experimental values. Interpolated temperature profiles at x/d=6 are compared with the experimental profiles in the adjacent sections.
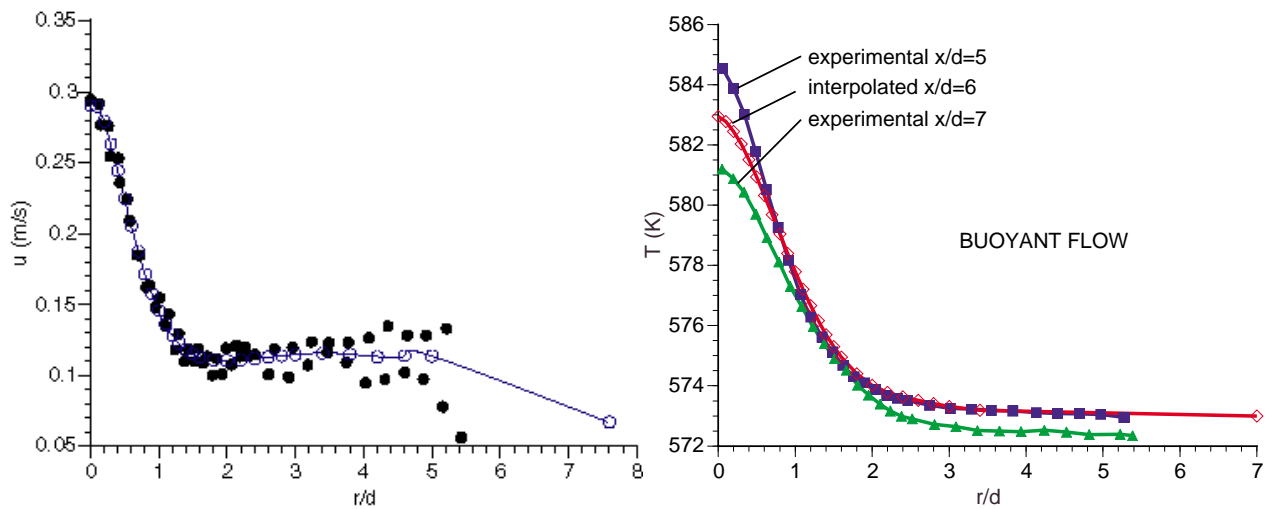

Figure 4 - Inlet velocity (left) and temperature (right) profiles for case b (buoyant flow). Solid symbols refer to actual experimental values. Interpolated temperature profiles at x/d=6 are compared with the experimental profiles in the adjacent sections.
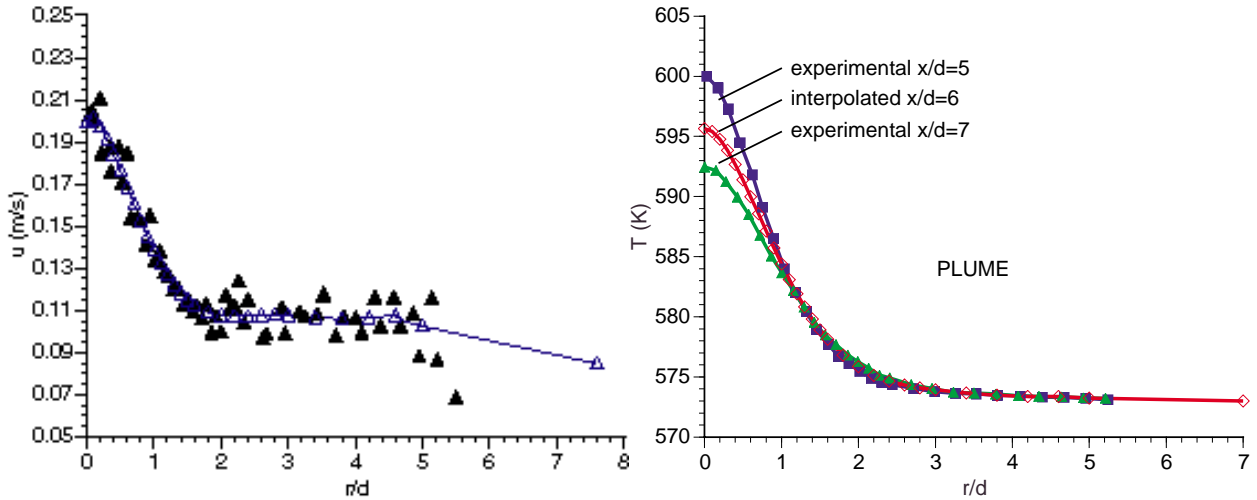
8

Figure 5 - Inlet velocity (left) and temperature (right) profiles for case c (plum). Solid symbols refer to actual experimental values. Interpolated temperature profiles at x/d=6 are compared with the experimental profiles in the adjacent sections.
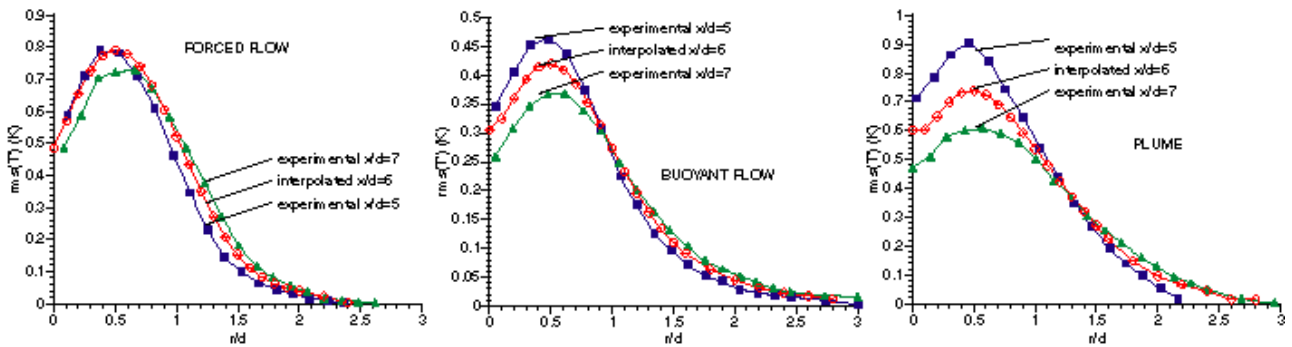

Figure 6 - Inlet profiles for temperature fluctuations. Interpolated temperature profiles at x/d=6 are compared with the experimental profiles in the adjacent sections.

Inlet turbulence kinetic energy profiles have been deduced by similitude with the experiments performed by Corrsin on a round jet of air [6], namely

$$k_{Na}(r) = k_a(r) \frac{\bar{u}_{Na}^2(r)}{\bar{u}_a^2(r)}$$

where the subscripts Na and a refer to sodium and air respectively and $\bar{u}$ indicates the inlet normal velocity. This procedure, based on the similarity of the turbulence fields in the cases of sodium and air for Reynolds numbers of the same order, is the more incorrect the more buoyancy effects become important. However, it have been be applied also to cases b) and c).

The problem of the inlet profile of the turbulence dissipation is more delicate, and can been considered one of the topics of the benchmark exercise. Two possible methods have been proposed. The first is based on the deduction of the ϵ profiles from the k profiles and the relation between the turbulent viscosity, k and ϵ

$$\nu_t = c_\mu \frac{k^2}{\varepsilon}$$

where $c_\mu = 0.09$ and a mean value of ν_t is deduced from the air experiments with similarity considerations. The ε profiles so obtained were modified on the basis of calculations performed at FZK, in order to obtain a correct inlet momentum flux. The resulting k and ε profiles are shown in Figure 7.
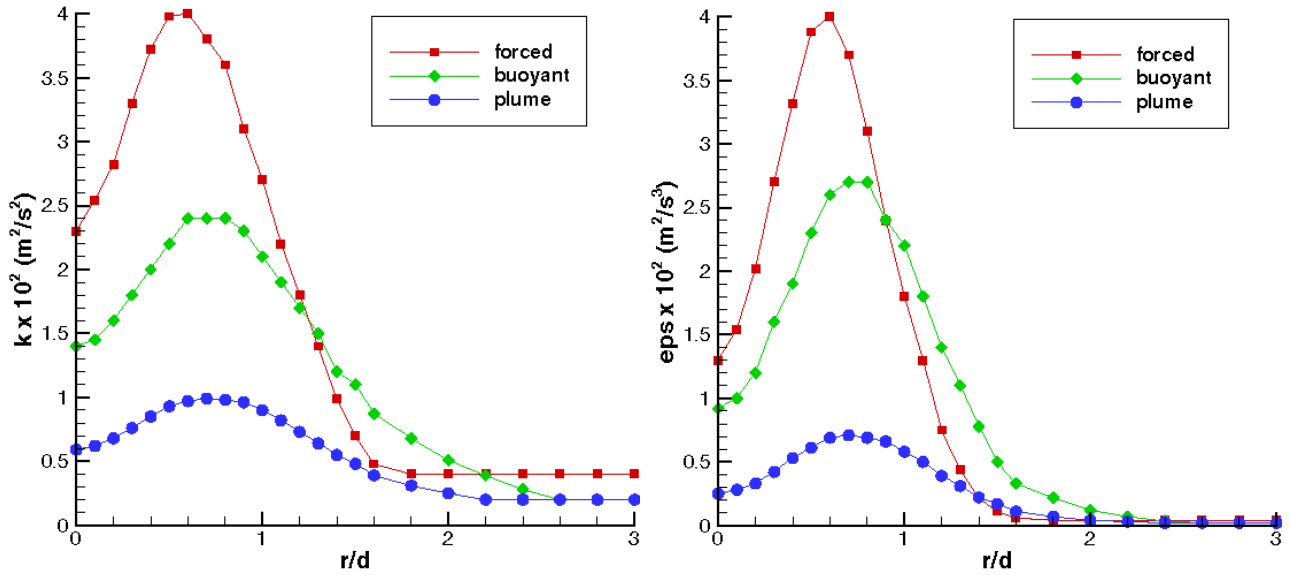

Figure 7 - Turbulent kinetic energy profiles deduced from [6] and corresponding dissipation inlet profiles deduced with the assumption of constant eddy viscosity.

An alternative is the application of a Neumann boundary condition for the turbulence dissipation, extrapolating the value of the first inner cell layer onto the boundary face. This corresponds to the application of

$$\left.\frac{\partial\varepsilon}{\partial n}\right|_{inlet} = 0$$

where n is the normal to the inlet plane. In this way, the inlet values of ε are determined by the inlet profiles of u and k, with the condition of no ε flux. Although this condition is not completely correct for this case (it is correct for example for a developed boundary layer in a pipe), it could give reasonable results, also considering that the ε production term generated by the velocity gradients could be dominant with respect to the inlet ε flux.

Both solutions for the ε inlet condition have been adopted within the the benchmark exercise. An alternative solution for turbulence boundary conditions has also been proposed by ENEA (see Sec. 5.3 and Appendix A3).

Concerning the inlet conditions for the turbulence parameters, the following points should be taken into account:

- the inlet profiles for the turbulence kinetic energy have been deduced from experiments performed in 1943 on an air jet in stagnant fluid. The jet Reynolds number was 1.4×10^3. Some uncertainties lie in this procedure:

  – the determination of the section corresponding to the TEFLU x/d = 6 section is not straightforward (the decay of the centreline velocity is different in the two cases). Anyway, only measurements in sections at x/d = 5, 10, 15, 20, 30, 40 are reported in the Corrsin paper.

  – Detailed profiles are available only for the axial component of the velocity fluctuations. Some assumptions are necessary for the other two components.

  – The jet Reynolds number is not the same. Being relatively low, it could have an influence on the turbulence levels.

- The inlet profiles for the turbulence dissipation have been deduced using a constant mean value of the turbulent viscosity along the inlet section, and scaling the so obtained profile on the basis of numerical experiments.

4. Strategy

The main task of the benchmark is the assessment of the limitations of an eddy viscosity approach for HLM flows. Some difficulties arise from the fact that the problems deriving from the HLM peculiarities are superimposed to the standard limitations of turbulence models. Furthermore, the problems related to the above-mentioned uncertainties in the boundary conditions must be taken into account. It should also be considered the fact that different commercial codes can give different results even if using the same turbulence models [7].

The codes available for the simulation are CFX, FLUENT, FLOW-3D, FLUTAN, KARALIS and STAR-CD. The codes and turbulence models used by each participant for the benchmark exercise are listed in Table 3.

Working group	Code	Turbulence modelling
CRS4 - EA	Star-CD	Chen k-ε, Standard k-ε (linear, quadratic and cubic), RNG k-ε
CRS4 - CFDC	Karalis	Spalart-Allmaras
ENEA	CFX	Menter k-ω, RNG k-ε, Low-Re k-ε
FZJ	Fluent	Standard k-ε, RNG k-ε, Spalart-Allmaras
FZK - IRS	Flutan	Standard k-ε, TMBF (k-ε + turbulent heat fluxes transport equations)
LAESA	Star-CD	RNG k-ε
NRG	Star-CD	Low-Re quadratic k-ε + Suga cubic model for turbulent heat fluxes
UPV	Fluent	Standard k-ε

Table 3 - Codes and turbulence models used for the TEFLU benchmark.

5. Results

The comparison between computational and experimental results have been carried out by comparing radial and axial profiles of velocity temperature and temperature fluctuations (when solved). Three cross sections were selected for radial profiles at a distance from the jet x/d=12, 20 and 40 for velocity profiles, and x/d=11, 19 and 39 for temperature and temperature fluctuation profiles. The decay of velocity and temperature along the centreline were also considered.

A summary of the approach and of the main results obtained by the benchmark participants is reported below. The complete reports can be found in the Appendix. In the following, figures and tables numbers refer to the corresponding document.

5.1. CRS4 - CFDC (Appendix A2)

Computations were performed using the CFD in-house developed code Karalis. Karalis is a parallel MPI, Finite-Volume, multi-block CFD code which solves the fully compressible Euler and Navier-Stokes equations with arbitrary thermodynamics. Although buoyancy effects are probably negligible in case A (table 2), under consideration here, buoyant forces were taken into account in the simulations. The Spallart & Allmaras one-eq. turbulence model was used for the computations.

As first step to the calculations proposed by the benchmark promoters, the entire domain sketched in figure 1 was simulated by imposing inlet step profiles for velocity and temperature, taking the values for jet and co-flow according to case A in Table 2. Different boundary conditions (both Dirichelet and Neumann) were tried in order to confirm the experimental curves at x/d=6. The best agreement was obtained using a value of $7.5\ 10^{-5}$ for the modified turbulent kinematic viscosity. The same order of magnitude can be derived from the air experimental data of Corrsin[3] by similarity considerations. The turbulent Prandtl number Pr_t was fixed to 1.3.

Following the prescriptions of the benchmark promoters, the computational domain was restricted from x/d=6(inlet) to x/d=61.5. The inlet boundary conditions were the regularized experimental data of velocity and temperature in section x/d=6.

The comparison between experimental and numerical velocity profiles at various sections is shown in figure 6. The great dispersion of data relative to section x/d=12 renders any quantitative comparison in this section very difficult. For the other sections (x/d=20,40) the most relevant fact is an overestimation in the jet region (r<10 mm), due obviously to an underprediction of turbulent viscosity by the turbulence model. In any case, it should be stressed that the qualitative distribution of turbulence viscosity in the domain seems to be very reasonable, giving maxima where the vorticity is higher.

By the opposite, a global underestimation of temperatures can be clearly observed in figure 7. As mentioned earlier, this fact could be due to higher values of Pr_t required by liquid sodium at these Reynolds numbers.

5.2. CRS4 - EA (Appendix A3)

The greatest part of the work was carried out on the forced-flow case. It was then shown that the main conclusions could have been applied to the buoyant and plume regimes as well.

Extrapolation inlet boundary conditions were adopted for the turbulence dissipation, considered more reliable especially in cases *b* and *c*. It was shown that, in case *a*, the results obtained with the two options for the ε inlet boundary were equivalent (Figure 4).

A comparison among different k-ε turbulence models implemented in Star-CD was carried out. A precise answer about the capability of such models at simulating the correct jet velocity field cannot be deduced, due to the uncertainties in the inlet turbulence boundary conditions. However, the Chen k-ε showed the lowest tendency to over-predict the jet spreading-rate (Figure 7).

In order to study the effect of the variation of Pr_t on the temperature profiles, the inlet turbulence kinetic energy profile was scaled in order to obtain a good agreement between calculated and experimental velocity profiles (Figure 9). Then, the value of Pr_t was changed from the standard value of 0.9 to 10 (on the basis of a formula proposed by Jisha and Rieche, page 13) and to 10^4 (to exclude the contribution of the turbulent heat transfer). A very good agreement with experimental measurements was found in both cases, the best being the case of no turbulent heat transfer (Figures 11-15). The above results indicate that the heat conduction is predominant in all flow regimes. In this situation, the standard value 0.9 of Pr_t yields an overestimation of the thermal diffusion rate.

On the basis of the results obtained in the forced-flow case, the cases of buoyant flow and plume were simulated, obtaining substantially the same results (Figures 16-23).

From the above results, nothing can be said about the validity of the Reynolds analogy for this kind of flow. However, even in the case it can be applied, a turbulent Prandtl number of order 1 is unsuitable for low-Reynolds-number flows of low-Prandtl-number fluids (low Peclet number flows).

5.3. ENEA (Appendix A4)

The simulation of the hot sodium jet-flow cases prescribed in the TEFLU benchmark was carried out using the CFX4 code. Calculations were carried out for the three flow regimes differing by the influence of the buoyant forces. The velocity, temperature and the different turbulent quantity fields, including the Reynolds shear stresses and the correlations of the velocity-temperature fluctuations, were calculated. The comparisons with the experimental results obtained for the same regimes of the hot sodium jet in the co-flow were given. Three different turbulence models were used and compared: Menter modified $k-\omega$, RNG and low-Reynolds-number $k-\varepsilon$.

The main output of the calculation campaign can be outlined in the following points:

1. The simulation of the jet-flow case prescribed in the TEFLU benchmark was fulfilled using the Menter modified $k-\omega$ turbulence model.

2. In general the calculations confirm the Gauss form of the radial distributions for the velocity and the temperature.

3. The velocity axial distributions calculated lie essentially below the experimental ones in the case of the forced jet and much below in the buoyant jet and plume cases. It occurs because the two equation turbulence models used, produce overestimated eddy viscosity values under the boundary conditions prescribed.

4. The temperature axial distributions calculated lie essentially below the experimental ones in the forced jet case and agree well enough (in spite of the large divergence in the velocity axial distributions) with the experimental values in the buoyant jet and plume cases. This occurs because of the inlet heat-flux balance lack.

5. Correcting the inlet heat fluxes and the turbulent quantity boundary conditions, a good agreement has been achieved between the calculated and experimental axial velocity and temperature distributions.

6. In the case of the jet-flow simulation, the low-Reynolds-number k-ε turbulence model gives a result in better agreement with the experiment, in comparison with the Menter modified k-ω turbulence model.

Generally speaking it is evident the strong influence of the type of turbulence k-e model used in the calculations. Moreover, it must be considered also the fact that, in the case of HLM, the turbulence heat transfer is of minor importance respect to the conductive heat transfer.

In this last case, it is not appropriate to adopt the default turbulent Prandt number (0.9) for the calculations, but a larger value should be used.

5.4. FZJ (Appendix A5)

The main task of FZJ within this work-package of the ASCHLIM project was to compare results achieved with the standard k-ε model for all three cases (forced jet, buoyant jet and plume) with those for the Spalart-Allmaras model. The CFD code Fluent was used for all calculations.

For the forced jet the spreading rate of velocity and temperature is overestimated in the calculations, while the results for the buoyant jet and the plume already agree quite well with the experimental results for the given boundary conditions. The spreading rate for the buoyant jet is slightly overestimated and that for the plume is lightly underestimated by the calculation. It can be assumed that this effect is based on improper boundary conditions regarding the turbulence at the inlet of the calculation domain. A good agreement between the standard k-ε model and the experiment can be achieved for all three cases with a slightly modified inlet-profile for the turbulent kinetic energy. The used multiplier for the forced jet is 0.7, for the buoyant jet 0.9 and for the plume 1.2.

The comparison of the results for the k-ε and the Spalart-Allmaras model with the experimental results has shown, that the spreading rate is predicted better by the k-ε model than by the Spalart-Allmaras one-equation model. The Spalart-Allmaras model seems to overestimate the production of turbulence along the centreline of the jet and slightly underestimates the production of turbulence in the wall regions.

In addition the effect of the turbulent Prandtl number was studied. It was found that higher values for Pr_t lead to better results regarding the temperature spreading rate for all investigated flow regimes. This denotes that for a standard value of approximately 1 the turbulent heat transfer is overestimated by the code. Good results can be achieved, if it is assumed that thermal conduction dominates the effect of turbulent heat transfer. It was also found that regarding the temperature spreading rate better results are achieved for the RNG k-ε model than for the standard k-ε model with the standard value of 0.85 for the turbulent Prandtl number. The main reason for this effect seems to be the differential equation for turbulent viscosity in the RNG k-ε model for low-Reynolds-number flows and the reduced value for the constant Cμ for high-Reynolds-number flows.

5.5. FZK - IRS (Appendix A6)

FLUTAN calculations of the turbulent hot jet of sodium are performed for all three different buoyancy regimes [12]. This type of flow has the advantage that the calculated turbulent mixing

will only depend on the turbulence models used, and perhaps also on the numerical schemes, but not on any wall models like wall functions. Two different turbulence models are applied: the standard k-ε-σ$_t$ model and a combination of a standard k-ε model with a full second order heat flux model called Turbulence Model for Buoyant Flows (TMBF) [2],[12].

Due to computational limitations, the flow in the multi-bore jet block was not discretised; thus, the results will depend heavily on the inlet conditions into the computational domain, which begins within the spreading area of the multi-jet arrangement. Here, we used widely the specified inlet conditions so that solely the influence of the different turbulent heat flux models can be analysed.

The calculations with FLUTAN with the k-ε-σ$_t$ model show the limits of the applicability of the eddy diffusivity approach in liquid metal flows. Whereas the calculated velocity fields are in close agreement with the measurements, the calculated temperature profiles are only in those cases acceptable in which the heat fluxes are more or less governed by the molecular diffusivity.

The TMBF which is a compromise between a classical low-Reynolds number k-ε-σ$_t$ model and the Reynolds stress model is an improvement of the k-ε-σ$_t$ model for turbulent flows in which the turbulent transport of heat is complex and the Reynolds analogy is not valid, such as in liquid metal flows. The TMBF allows for analysis of the local turbulent Prandtl number. The results show, that values between two and five occur, and that a complex spatial distribution of the turbulent Prandtl number builds up, so that any concept basing on Reynolds analogy would need non-constant values to reproduce the required turbulent heat fluxes.

In all cases, the temperature fields calculated by the TMBF model agree better with the measured data. The TMBF does already contain some specific model extensions which were deduced from direct numerical simulations for turbulent liquid metal convection [8]. Further improvements of the TMBF are still necessary for liquid metal flows to reduce the overestimation of the radial profiles of T'^2 in the plume regime. The inclusion of the Peclet number dependency in the transport equation of ε$_{T'}$ [10],[11] should lead to physically sound results.

Even though the FLUTAN predictions agree well with experimental data, further validation of the TMBF is needed especially for liquid metal flow regimes where the velocity field is mainly determined by turbulent heat transport.

One should keep in mind that the range of validity of the TMBF could be restricted by the assumption of isotropy of the eddy viscosity ν$_t$ whereas anisotropy is included in the calculated turbulent heat fluxes. Such anisotropy in the eddy viscosity may become important in 3-D flows, in strongly buoyant flows, and near walls. For these kinds of flows, at least Algebraic Stress Model (ASM) extensions for the two-equation shear stress models should be used in addition. Such a model would combine the necessity of having the possibility to include anisotropic eddy diffusivities and an accurate heat flux modelling together with an acceptable numerical effort and robustness.

5.6. LAESA (Appendix A7)

We have simulated the forced jet case in the TEFLU experiment with the RNG k-ε model implemented in StarCd. We have shown the set of equations that the code solved in order to find out the solution, and which are de coefficients associated to these equations. The results of the calculation shows that the model is able to fit very well the experimental data corresponding to the temperature profile. Nevertheless, the velocity profiles obtained are quite far from experimental data. In order to explore the possibilities of the model to further calculation of this kind of problems, we have performed sensibility studies of the results to modifications of the model

coefficients. We have realised that we can approach to the experimental data by changing $C_{\varepsilon 1}$ and $C_{\varepsilon 2}$. In any case, new values for these parameters suggest that the standard or Chen k-ε model might be more suitable for the treatment of this kind of problems.

5.7. NRG (Appendix A8)

The NRG contribution was mainly dedicated to investigate whether an advanced model for the turbulent heat flux contributes to an improved temperature calculation in heavy liquid metal turbulent jet flows.

At the inlet, the axial velocity, turbulent kinetic energy (k), turbulent dissipation rate (_) and temperature have been prescribed. The profiles are provided by the TEFLU proposal.

The low-Reynolds number k-_ model of Lien, Chen and Leschziner has been used in the calculations. In conjunction with this model, the non-linear model of Suga has been used as constitutive relation for the turbulent heat flux. Suga's model is intended to be used in conjunction with non-linear constitutive relations for the turbulent stresses. For the turbulent stresses, the quadratic turbulence model has been used.

The results of the three cases (forced jet, buoyant jet and plume) are similar. The calculated jet spreading is faster than the experimental spreading. The calculated velocities and temperatures in the jet region are lower than the experimentally observed velocities and temperatures. The velocity and temperature profiles show so-called self-similarity. However, the shape of the inlet profiles deviates from the shape of the profiles further downstream. This is an indication that the inlet boundary conditions are not correct.

The main result is that the jet in the calculation spreads faster than in the experiment. This implies that the calculated velocity field deviates from the experimental field. Also the calculated temperature field deviates from the experimental field. Therefore, on the basis of this comparison, it cannot be concluded whether the advanced model of Suga for the turbulent heat flux contributes to an improved temperature calculation in heavy liquid metal turbulent jet flows.

5.8. UPV (Appendix A9)

The contribution of UPV/EHU to this work-package is the use of the standard k-ε turbulent model of FLUENT. The inlet profiles (velocity, temperatures, turbulent kinetic energy and dissipation of the turbulent kinetic energy) used are the one indicated in the proposal of this work-package.

Radial velocities and temperatures profiles show a very good agreement with the experimental results. However, it is observed that smaller velocities and temperatures are predicted in the centerline of the domain. So, calculations with the standard k-ε model predict that the jet is spreading inside the tube quicker than the experimental results.

Taking into account the three different cases, temperature profiles are better predicted in the plume flow, while the worst is the forced-jet case. Velocity profiles, however, present better agreement if the flow is forced. In the plume case, the axial velocities are over predicted. In general, both the temperature and the velocity variables are better predicted if the flow is buoyant.

Apart from this contribution, and in order to compliment it, calculations with some other FLUENT turbulence models have been made (Spalart-Almaras (1 equation. model), standard and RNG k-ε and Reynolds stress model (RSM)). These calculations show a better approximation to the experimental results if they are made by the RNG k-ε and RSM models (no difference between them). The 1 equation model shows a very good agreement in the temperature profile, but the

velocities are overestimated. The calculation of the turbulent viscosity is the main issue for these results..

On the other hand, there are not good results with LES model in a 2D problem, as turbulence is a 3D phenomenon.

6. Conclusions

The TEFLU benchmark was chosen to investigate the performance of current turbulence models including turbulent heat flux modelling, because it allows to investigate the performance and abilities of the models in liquid metal flows with heat transfer independent of any wall conditions. In addition it should allow to consider their performance and deficiencies in different buoyancy flow regimes. From the results reported above, the following conclusions can be drawn for the TEFLU benchmark.

1. No experimental measurements of velocity fluctuations were available. Furthermore, due to computational limitations, none of the participants did discretise the flow in the multi-bore jet block. Therefore, the mixing or spreading results will heavily depend on the turbulence level specified in the inlet conditions into the computational domain, which begins within the spreading area of the multi-jet arrangement. For this reason, it was not possible to draw absolute conclusions about the capability of turbulence models to predict the correct jet spreading-rate. Some inlet conditions were specified in the benchmark description, which allowed the relative deviations between different turbulence models to be analysed. It should be also noted that, in order to limit the analysis to the turbulent heat transport, some of the participants used also scaled inlet conditions to obtain correct velocity spreading rates.

2. The velocity spreading-rate obtained with the prescribed inlet turbulence profiles is overestimated in the forced-flow regime. This result is confirmed by all participants but CRS4-CFDC (using a Spalart-Allmaras model) and LAESA (RNG k-ε). Better results are obtained in the buoyant and plume regimes if the assigned profile of ε are used (FZJ, FZK, UPV), while even worse results are obtained by using the extrapolation condition (CRS4-EA, ENEA, NRG). The reason of it can be found both in the bad performance of two-equation models at predicting round-jets, and in inadequate inlet turbulence boundary conditions. A comparison between various versions of the k-ε models implemented in Star-CD showed that the Chen k-ε predicts the lowest jet spreading-rate.

3. The temperature spreading rate is overestimated by all models based on the Reynolds analogy, using $Pr_t = 0.9$. The error is higher in the forced flow regime. Good results are obtained with the TMBF model (FSZ-IRS), which solves equations for the turbulent heat fluxes, and by LAESA. In this last case, it could be due to the strong underestimation of the turbulence field, as it can be deduced from velocity results.

4. The comparison between the molecular and the turbulent heat diffusion coefficients calculated with the Reynolds analogy ($Pr_t = 0.9$, CRS4-EA) and with the TMBF model (FZK-IRS), shows that they are of the same order of magnitude, with a prevailing effect of thermal conduction. The value of Pr_t calculated from TMBF results ranges from 2 to 5. However, CRS4-EA obtained the best agreement for temperature profiles with $Pr_t = 10^4$, namely considering only thermal conduction, which would lead to the conclusion that the turbulent heat transfer plays a negligible role in the jet temperature spreading. Definitely, we can conclude that a correct temperature spreading rate can not be obtained using a Pr_t approach with $Pr_t \sim 1$. A more critical check of the other models should be repeated for a flow at larger Reynolds numbers, in which the turbulent heat transfer is more relevant than the molecular one.

5. The buoyancy influence on the turbulent heat transport was found to be only weak in all TEFLU experiments. So, definite conclusions on the validity of the investigated models for

strongly or purely buoyant liquid metal flows can not be drawn from this analysis. From the experience with other fluids it is known that for such flows models are required which record the anisotropy in the turbulent momentum fluxes and which use at least a transport equation for the temperature variances to model thermal stratification phenomena.

7. References

[1] J. U. Knebel et al., "Experimental investigation of a confined heated sodium jet in a co-flow", *J. Fluid Mech. (1998), vol. 368, pp. 51-79.*

[2] D. C. Wilcox, "Turbulence Modelling for CFD", DCW Industries, Inc., 1994.

[3] Y.S. Chen, S.W. Kim, "Computation of turbulent flows using an extended k-ε turbulence closure model", NASA CR-179204, 1996

[4] "Star-CD v3.05 User Manual", *Computational Dynamics Limited, 1998.*

[5] "FLUENT 5 User's Guide Volume 2", *FLUENT Incorporated, 1998.*

[6] S. Corrsin, "Investigation of flow in an axially symmetric heated jet of air", *NACA wartime report, W-94, 1943.*

[7] L. Maciocco et al., "Benchmark Calculation of Mercury Flow Experiments Performed in Riga for the ESS Target", *CRS4 Technical Report 99-21, 1999.*

[8] Carteciano, L.N., Wörner, M., Grötzbach, G., 1999. Erweiterte Turbulenzmodelle für technische Anwendung von FLUTAN auf Naturkonvektion. Jahrestagung Kerntechnik 99, Karlsruhe, May 18-20, pp.129-134.

[9] Carteciano, L.N., Weinberg, D., Müller, U., 1997. Development and analysis of a turbulence model for buoyant flows. 4th World Conference on Experimental Heat Transfer, Fluid Mechanics and Thermodynamics. Bruxelles, June 2-6, Vol.3, pp. 1339-1347.

[10] Wörner, M., Grötzbach, G., 1996. Analysis of the transport equation of temperature variance dissipation rate by direct numerical simulation data of natural convection. Engineering Turbulence Modelling and Experiments 3, Eds.: W. Rodi, G. Bergeles, Elsevier Science B. V., pp. 229-238.

[11] Wörner, M., Ye, Q.-Y., Grötzbach, G., 1999. Consistent modelling of fluctuating temperature-gradient-velocity-gradient correlations for natural convection. Engineering Turbulence Modelling and Experiments 4, Eds.: W. Rodi, D. Laurence, Elsevier Science B. V., pp. 165-174.

[12] Carteciano, L.N., Grötzbach, G., 2003. Validation of turbulence models for a free hot sodium jet with different buoyancy flow regimes using the computer code FLUTAN. Forschungszentrum Karlsruhe, FZKA 6600.

Appendix A1.

Author(s): **L. Maciocco**
Company: **CRS4**
Title: **Proposal for the benchmarking activity on the TEFLU sodium jet experiment**
Date: **15 September 2000**

Appendix A2.

Author(s): **I. Di Piazza, M. Mulas**
Company: **CRS4**
Title: **Numerical simulation on the TEFLU sodium jet experiment using the CFD code Karalis**
Date: **7 November 2000**

Appendix A3.

Author(s): **S. Buono, L. Maciocco, V. Moreau, L. Sorrentino**
Company: **CRS4**
Title: **CFD simulation of a heated round jet of sodium (TEFLU benchmark)**
Date: **17 July 2001**

Appendix A4.

Author(s): G. Mercurio, V.V. Anissimov, V.I. Mikhin, Y.I. Gritsaev
Company: ENEA-IPPE
Title: ENEA-IPPE benchmark activity on the TEFLU sodium jet experiment
Date: 4 July 2001

Appendix A5.

Author(s): J. Wolters
Company: FZJ
Title: Benchmark activity on the TEFLU sodium jet experiment
Date: March 2002

Appendix A6.

Author(s): **L.N. Carteciano, G. Grötzbach**
Company: **FZK-IRS**
Title: **Calculations for the TEFLU sodium jet benchmark with the computer code FLUTAN**
Date: **16 February 2001**

27

Appendix A7.

Author(s): A. Abanades, A. Castro.
Company: LAESA
Title: Simulation of the forced jet flow case of the TEFLU experiment in LAESA
Date: January 2002

Appendix A8.

Author(s): **N.B. Siccama, E.M.J. Komen, H. Koning**
Company: **NRG**
Title: **Post-Test CFD analysis of the TEFLU sodium jet experiment**
Date: **20 September 2001**

Appendix A9.

Author(s): **A. Peña, J. Merino, A. Etxegia**
Company: **UPV**
Title: **Results of the simulation of the TEFLU experiment**
Date: **16 November 2001**